

# Thermal gradient induced sidebranching in directional solidification

M. Georgelin<sup>a</sup> and A. Pocheau<sup>b</sup>

IRPHE<sup>c</sup>, Universités Aix-Marseille I & II, Faculté de Saint-Jérôme, S.252, 13397 Marseille Cedex 20, France

Received: 22 December 1997 / Revised: 31 March 1998 / Accepted: 2 April 1998

**Abstract.** The effect of thermal gradient on sidebranching is studied experimentally in directional solidification of impure succinonitrile. An experimental procedure capable of changing thermal gradient while keeping pulling velocity *and* cell-spacing constant is applied. It enables us to directly observe the effect on sidebranching of the *sole* change of thermal gradient. It is found that increase of thermal gradient enhances sidebranch amplitude and reduces sidebranching onset.

**PACS.** 81.30.Fb Solidification – 68.70.+w Whiskers and dendrites (growth, structure, and nonelectronic properties) – 47.20.Hw Morphological instability; phase changes

## 1 Introduction

Sidebranch emission by growth cells stands as one of the most spectacular dynamical event of solidification processes. In view of its practical consequences on solidified alloys and of its fundamental challenge, a long standing effort has been devoted to clarify its mechanism. Nevertheless, important open questions remain as to the origin of sidebranches, especially in directional growth: Do they refer to a jump of branches of solution relevant to growth cells [1,2] or to dynamical features displayed on a definite branch [3]? In this respect, what is the nature and the main features of cell branch [2,4,5]? Finally, is the phenomenon of sidebranching relevant to an attractor of a dynamical system [3] – according to which sidebranching cells, so-called dendrites, would stand as oscillators – or to a mesoscopic extrapolation of noise [6] – according to which they would stand as noise amplifiers?

These questions have been addressed in literature, both for free growth (growth in a uniformly undercooled melt) and for directional growth (growth in imposed thermal gradient). In the former case, a number of well-controlled experiments [7,8] and detailed theoretical analysis [9,10] have been performed. They have concluded that sidebranching refers to noise amplification of disturbances at the course of their advection down the side of needle crystals which forms are selected by surface tension anisotropy [8,10]. By comparison, in directional growth, neither theory nor experiment have been pushed at the level of details reached in free growth, in spite of some detailed studies [1,11]. Yet, thermal gradient seems to open

new problematic as to the branch of solution pertaining to growth cells [2,4,5]. Depending on the nature of the growth branch, this could result in sidebranching mechanism different than that involved in free growth. For this reason, sidebranching deserves further investigation in the directional case, both on the experimental and theoretical grounds.

To improve the study of sidebranching in directional solidification, we have recently performed an experiment in which cell-spacing  $\Lambda$  was uniform enough along the front to be considered as an effective control parameter [12]. Then, a picture different than that deduced by using average cell-spacings [1,13] emerged: the control parameter space  $(V, \Lambda, G)$  splits into two domains, one involving steady cells, the other referring to sidebranching. The surface separating them corresponds to sidebranching onset. Interestingly, the dependence of this “critical surface” on control parameters points to a striking feature: raising thermal gradient should promote sidebranching [12]. This means that increasing thermal gradient should destabilize cells with respect to sidebranching, in surprising contrast with its well-known stabilizing action with respect to the primary instability responsible for cell formation.

The purpose of this paper is to *directly* test the prediction of thermal gradient induced sidebranching in directional solidification of impure succinonitrile. For this, an experimental procedure is designed so as to noticeably change thermal gradient on a given front, while keeping the remaining control parameters, pulling velocity but *also* cell spacing, constant.

Experimental set-up and characterization of the critical surface for sidebranching are reported in Section 2. The experimental issue of thermal gradient change and the observed effect on sidebranching are addressed in Section 3. Discussion on the meaning of thermal

---

<sup>a</sup> e-mail: georgel@lrc.univ-mrs.fr

<sup>b</sup> e-mail: pocheau@lrc.univ-mrs.fr

<sup>c</sup> UMR 6594 CNRS

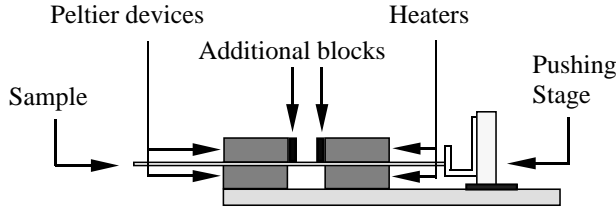


**Fig. 1.** Sketch of experimental set-up. Small thermal blocks have been added so as to change thermal gradient by simply removing them.

gradient induced sidebranching is reported in Section 4 and a conclusion about this work is drawn in Section 5.

## 2 Experiment and critical surface

### 2.1 Set-up and procedure

The experimental set-up, described in detail in [12], follows from the principle drawn by Jackson and Hunt [14]: a thin sample of mixture is mechanically pushed in a thermal gradient generated by heaters and coolers (Fig. 1). Special care has been taken to minimize mechanical and thermal perturbations and to select crystal orientation.

Sample translation is provided by a linear ball-screw driven stage monitored by a micro-stepper motor and controlled by Michelson interferometry. Relative accuracy of pulling velocity  $V$  is  $\delta V/V = 3\%$  over a screw pitch. Heaters (resp. coolers) are made of metallic blocks, 1 cm thick,  $5 \times 5 \text{ cm}^2$  wide in close contact with a resistance sheet (resp. Peltier device). Both are electronically regulated to better than  $10^{-1} \text{ K}$ . They are separated by a gap  $g$  which can be varied from 5 to 20 mm. An exploded optical set-up providing large frontal distances has been preferred to a microscope so as to preserve, around the front, a large zone free of instrumental disturbance. Magnifications from 2 to 40 are available.

Samples are made of two glass plates, 45 mm large, 100 mm long, sandwiching 100  $\mu\text{m}$  thick spacer sheets and filled with nominally pure succinonitrile purchased from Sigma Chemical Co, St Louis. To get rid of end-effects, only a few millimeters wide central region, far from sample boundaries, is studied. A NMR study reveals that the dominant impurity is presumably ethylene. Solutal diffusivity in the liquid phase,  $D$ , and partition coefficient,  $k$ , have been deduced from measurements of relaxation time of planar front to equilibrium, critical velocity, melting temperature and solidification temperature:  $D \approx 1.0 \pm 0.5 \times 10^{-5} \text{ cm}^2\text{s}^{-1}$ ,  $k = 0.3 \pm 0.05$ .

In order to inhibit spurious dynamics generated by cell instability, cell interaction, grain boundary and anisotropy, care has been taken to select large monocrystal domains with crystalline axis parallel to pulling velocity (*i.e.* to thermal gradient), cell depth or mean front direction. Observations of the growth direction of dendrites at large velocities showed that fluctuations of crystal orientation are smaller than 3 degrees over at least

a hundred cells. According to this, no frustration induced by a conflict of growth direction [15] occurred, nor was the pattern disturbed by grain boundary motions. Accurate selection of cell spacing could then proceed over long times to provide steady uniform states involving a definite cell spacing  $\Lambda$  and a definite crystalline orientation. In practice, cell-spacing extrema over front parts 3 mm long, *i.e.* about 30 cells, differ only by  $\Delta\Lambda = \pm 5 \mu\text{m}$ . Accordingly, spacing increments  $\delta\Lambda$  from one cell to its neighbour remained, in relative average, smaller than:  $\delta\Lambda/\Lambda < 5 \times 10^{-2}$ .

In the sequel, we shall denote  $V_c$  the critical velocity of the primary instability of planar fronts,  $m$  the liquidus slope,  $c_\infty$  the solute concentration far ahead from the front,  $d_0$  the capillary length ( $d_0 \approx 1.3 \times 10^{-2} \mu\text{m}$  here) and  $l_T \approx D/V_c$  the thermal length.

### 2.2 Critical surface for sidebranching

At fixed cell-spacing and thermal gradient, a given cell emit no sidebranch at low velocity but some at larger velocities. As shown in a previous study [12], it actually undergoes in between a *definite* cell-dendrite transition. This transition is characterized by an order parameter  $A$  taken as the maximal sidebranch amplitude over the cell and over the time. Then, cellular and dendritic states formally refer to  $A = 0$  and  $A > 0$  respectively. In between stands the critical surface for sidebranching where cells are marginally stable with respect to the sidebranching instability:  $A = 0^+$ . The fact that this critical surface could be actually observed means that the cell-dendrite transition is, for this order parameter  $A$ , supercritical.

The critical surface has been determined by a systematic study of the marginal states  $A = 0^+$  in the parameter space made by pulling velocity  $V$ , cell spacing  $\Lambda$  and thermal gradient  $G$ . Fitting it with power laws reveals the following scaling law (Fig. 2):

$$A = 0^+ \quad \text{for} \quad V \Lambda^2 G^{1/4} = C \quad (1)$$

where  $C$  only depends on mixture parameters, *i.e.*  $k$ ,  $D$ ,  $m$ ,  $c_\infty$  and  $d_0$ .

According to it:

$$\begin{aligned} V \Lambda^2 G^{1/4} > C &\Leftrightarrow A > 0 \Leftrightarrow \text{unstable domain} \\ V \Lambda^2 G^{1/4} \leq C &\Leftrightarrow A = 0 \Leftrightarrow \text{stable domain.} \end{aligned}$$

A striking feature of this critical surface is revealed by its implication on the evolution of sidebranching with control parameters: increasing either  $V$ ,  $\Lambda$  or  $G$  induces a transition from the stable domain to the unstable domain and thus promotes sidebranching. Following this conclusion, all the parameters  $V$ ,  $\Lambda$ ,  $G$  should be destabilizing with respect to sidebranching. This is well known for  $V$  and  $\Lambda$  but is quite surprising for  $G$  since at variance with its stabilizing role on planar fronts.

Although conclusive we emphasize, however, that this study of the critical surface refers not to a continuous

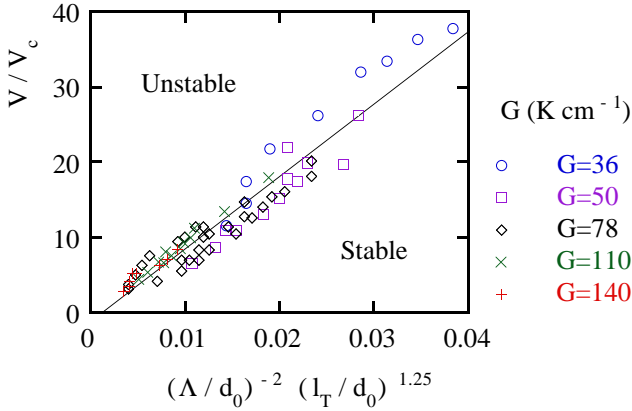


**Fig. 2.** Critical surface for sidebranching. Unstable domain referring to sidebranching emission is above; stable domain referring to no noticeable sidebranching is below. Here,  $d_0 \approx 1.3 \times 10^{-2} \mu\text{m}$ , and  $l_T \approx D/V_c$ . As  $V_c$  is proportional to  $G$ , this evidence of scaling law for the critical surface yields relation (1).

evolution with  $G$  of a *given* growth state, but to a compilation of *different* ones picked up at the transition to sidebranching. In this respect, the conclusion reached as to the destabilizing nature of  $G$  must be considered as *indirect*. Owing to its implication for the understanding of sidebranching, it thus calls for a *direct* confirmation on definite growth states. This is addressed below.

### 3 Thermal gradient induced sidebranching

We consider a cellular interface involving uniform cell spacing and crystalline principal axes aligned onto pulling direction, sample depth or mean front direction. In order to reveal the sole effect of  $G$  on sidebranching, change of thermal gradient must be performed so as to keep the remaining control parameters,  $V$  and  $\Lambda$ , fixed.

#### 3.1 Thermal gradient change

Two ways are available for changing  $G$ : one by modifying the temperature difference  $\Delta T$  between heaters and coolers; the other by varying the gap  $g$  between them. Our choice has been conditioned by two experimental constraints: keeping the cell-spacing  $\Lambda$  fixed; changing  $G$  sufficiently so as to induce a noticeable effect on sidebranching.

The former constraint especially requires triggering no cell instability as tip-splitting or cell elimination during the transient from one to another gradient, since cell spacing would evolve following pattern dynamics. To achieve this, cell position must be kept constant so as avoid modifying abruptly the effective growth velocity of the front or the effective shape of the solute concentration field, as seen from cells. In practice, this implies keeping the melting isotherm of cell tips fixed while changing thermal gradient.

The easiest way for changing  $G$  would have been to modify the temperature difference  $\Delta T$ . However, this could not be efficient because of limitations in temperature variations. In particular, the range of low temperatures provided by coolers is limited, on one hand by the power of the Peltier devices and, on the other hand, by the temperature of the water circulation used to remove heat from the cooling stage. Both restrict the available temperature variation in between  $8^\circ\text{C}$  and  $20^\circ\text{C}$ . The possible temperature change at the coolers is thus limited to only 12 K, *i.e.* 10% of the temperature difference  $\Delta T$ . Such a large restriction is not in order at the heaters whose temperatures may be changed at convenience from above the melting point of the mixture,  $56^\circ\text{C}$ , to about  $120^\circ\text{C}$ . However, as fronts roughly stand at medium distance between heaters and coolers, one cannot use this full temperature range if the melting isotherm of cell tips has to be kept fixed. Instead, one must pay attention to apply nearly opposite temperature variations to heaters and coolers so as to maintain their medium temperature unchanged. In this case, the available change of  $\Delta T$  is imposed by the coolers so that, in practice, the available relative change of thermal gradient is less than 20% at fixed gap: this is insufficient to point out a significant effect on sidebranching.

We have thus turned attention to a change of gap  $g$ . As this modifies the thermal configuration, a thermal shock on the front might be feared. However, as the change addresses not the temperature themselves, but the sources of heat, emission of strong thermal waves is reduced. In practice,  $g$  could be modified by a factor about 2, yielding, in the run described below, a thermal gradient change from  $105 \text{ K cm}^{-1}$  to  $60 \text{ K cm}^{-1}$ .

Additional precaution has to be taken to keep cell positions fixed, however. Indeed, as the thermal field is not only diffused but also advected by sample translation, it involves weak non-linear spatial variation according to which its gradient is, strictly speaking, *non-uniform* on the sample. Accordingly, even a symmetric change of temperatures of heaters and coolers would not maintain the mean temperature isotherm at a fixed location and, therefore, not the front either. In particular, we stress that, whereas the shift of temperature field from the conductive profile is zero at both heaters and coolers, it is nearly maximum at a medium distance from them, where the front is actually located. For this reason, the position of the solidification isotherm may be expected to be sensitive to a change of gap, even if this change is symmetric with respect to it (Fig. 1). To compensate its variation at the course of the transient to new thermal and solutal equilibrium, the remaining degrees of freedom, *i.e.* the temperatures of heaters and coolers, have to be monitored. By slightly adjusting them on a 4 K range, cell tip position could then be kept quasi-constant until equilibrium. This way, neither tip-splitting nor cell instability occurred, so that cell spacing could easily remain the same during thermal change.

To modify gap  $g$ , the most natural method would have been to translate heaters and coolers. This, however,

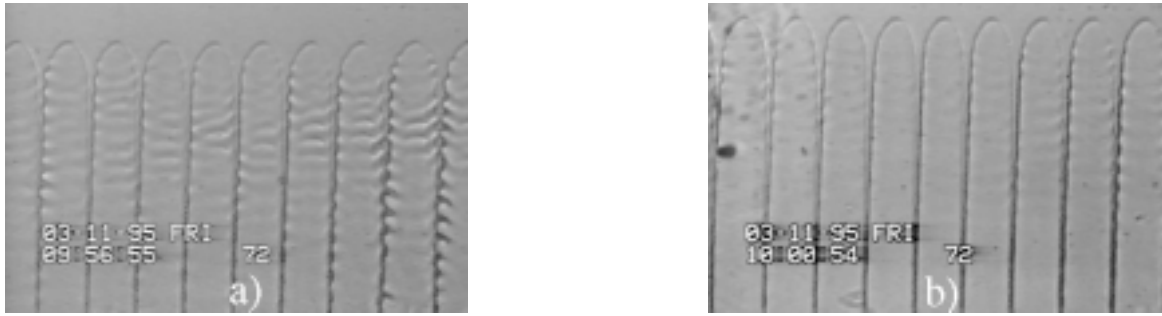


**Fig. 3.** Weakening of sidebranch emission by thermal gradient decrease: global view on many cells.  $V = 15.0 \mu\text{m s}^{-1}$ ,  $V_c = 1.45 \mu\text{m s}^{-1}$  at  $G = 78 \text{ K cm}^{-1}$ , view width  $1040 \mu\text{m}$ , (a)  $G = 105 \text{ K cm}^{-1}$ , (b)  $G = 60 \text{ K cm}^{-1}$ , 4 minutes, *i.e.* 4 thermal diffusion times  $\tau_t$ , later. Weakening of sidebranching is noticeable on both directions of sidebranch emission.

would have resulted, in our set-up, in large perturbations of contacts between sample and blocks and, finally, in large fluctuations of sample position. Another method has thus been chosen (Fig. 1): small additional blocks, in close contact with the basic blocks, have been introduced on the upper part of the sample, so as to artificially reduce gap. Increase of  $g$  could then simply be obtained by removing them. As this required no fine adjustment and could be achieved at once, this produced minimal perturbations on growth fronts. We note that  $G$  could only be decreased this way. This, however, does not prevent this method to fit with our purpose since, our goal being to compare asymptotic states at two different gradients irrespective of their succession in time, the sens of variation of  $G$  is irrelevant.

### 3.2 Transient / asymptotic regimes

Two different regimes have to be distinguished following the removal of additional thermal blocks: the transient accompanying the establishment of another thermal gradient; the asymptotic state reached at the new thermal gradient value. For our purpose, only the latter regime is relevant, provided that no change of other parameters, especially cell spacing, occurred during transient.

The transient time depends on the relaxation time of the thermal field,  $\tau_t$ , and on those relevant to the concentration field. As blocks were removed at both heaters and coolers, the former time,  $\tau_t$ , refers to thermal relaxation on a half-gap. According to measurements of thermal diffusivity of the sample,  $\kappa = 5 \times 10^{-3} \text{ cm}^2 \text{ s}^{-1}$ , and to the largest gap involved,  $g = 10 \text{ mm}$ ,  $\tau_t = g^2/(4\kappa)$  is about 1 min. Regarding the concentration field, two kinds of relaxation times are in order: that due to diffusion-advection of yet present impurities,  $\tau_d$ , and that involving the diffusion of impurities generated by the solidification process,  $\tau_i$ . The former,  $\tau_d$ , rests on perturbations induced by slight cell motions. As the fluctuations of cell position are maintained at values smaller than the cell spacing  $\Lambda$ , relaxation by diffusion or advection stands on time-scales lower than  $\Lambda^2/D$  or  $\Lambda/V$  respectively. These are however of the same order of magnitude, since Péclet numbers  $Pe = AV/D$  are

about unity here:  $\tau_d \approx \Lambda^2/D \approx \Lambda/V \approx 10 \text{ s}$ . Finally, the last relaxation time,  $\tau_i$ , is of order  $D/kV^2$ , since only a fraction  $k$  of solute is relaxed in the liquid at the course of solidification. Its value is about 30 s here.

Following these evaluations,  $\tau_t \approx 2\tau_i \approx 6\tau_d \approx 1 \text{ min}$ . Accordingly, a waiting time of a few minutes, *i.e.* several relaxation times, was required before addressing the asymptotic states of the system.

### 3.3 Sidebranching inhibition by thermal gradient decrease

Effects of decrease of thermal gradient on sidebranching at otherwise fixed parameters were found reproducible. Two typical runs are displayed in Figures 3a,b and 4a,b.

In Figure 3, the initial state (Fig. 3a) corresponds to  $G = 105 \text{ K cm}^{-1}$ . It shows noticeable sidebranches which, in agreement with the selected crystal orientation, take place on directions perpendicular or parallel to the sample plane. Then, thermal gradient has been reduced to  $60 \text{ K cm}^{-1}$  by removing the additional thermal blocks. The waiting time until observation has been 4 min, *i.e.*  $4\tau_t$ , but no relevant evolution was actually noticed at subsequent times. The final state, shown in Figure 3b, involves same cell-spacing, same pulling velocity but displays a significant decrease of sidebranch amplitude. In particular, the central cell is now even almost steady.

Figure 4 shows the same phenomenon on few cells. Here, in the initial state (Fig. 4a), sidebranches are emitted on a single direction. Their amplitude is large, especially in the grooves and sidebranch-induced distortions may even be noticed close to the tip. In Figure 4b, sidebranch amplitude is much smaller, following thermal gradient decrease. In particular, sidebranches are hardly visible close to the tip and are actually weak in the grooves.

These observations show that sidebranching has been weakened by thermal gradient decrease. As this statement refers to asymptotic states, its reciprocal is valid: increasing thermal gradient from Figures 3b, 4b to Figures 3a, 4a promotes sidebranching; thermal gradient enhances sidebranching.

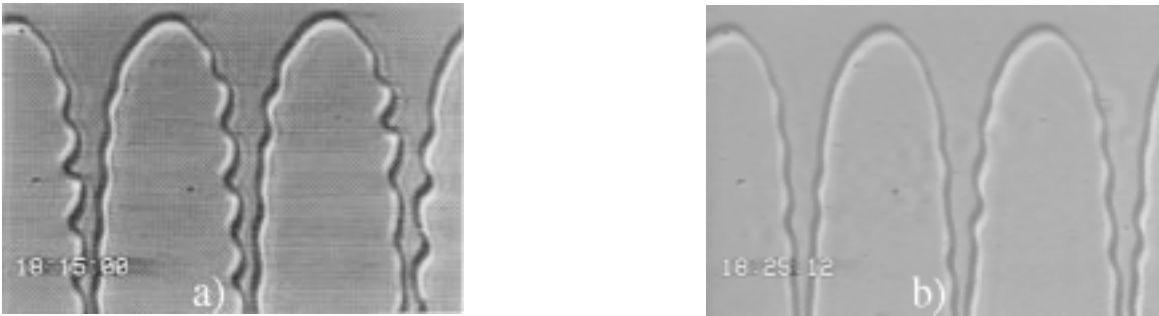


**Fig. 4.** Weakening of sidebranch emission by thermal gradient decrease: restricted view on few cells.  $V = 12.0 \mu\text{m s}^{-1}$ ,  $V_c = 1.78 \mu\text{m s}^{-1}$  at  $G = 78 \text{ K cm}^{-1}$ , view width  $520 \mu\text{m}$ , (a)  $G = 105 \text{ K cm}^{-1}$ , (b)  $G = 60 \text{ K cm}^{-1}$ , 10 minutes, *i.e.* 10 thermal diffusion times  $\tau_t$ , later. Weakening of sidebranching is noticeable on the direction of sidebranch emission.

## 4 Discussion

To analyze the role of thermal gradient in sidebranching, let us first recall the relevant growth phenomena in which thermal gradient is involved. There are basically two of them: primary instability of Mullins-Sekerka and cellular form. In addition, cellular form indirectly monitors both tangential advection along the sides of growth interface and cell position in temperature field, *i.e.* cell tip undercooling. As all these factors may participate in sidebranching mechanism, it is worth addressing for each of them, at least qualitatively, whether they favor or inhibit sidebranching, upon an increase of thermal gradient.

As increase of thermal gradient brings isothermal lines closer, equilibrium shapes should flatten. This is not apparent by comparison between Figures 3a, 4a and 3b, 4b but might be noticeable with better resolution or larger thermal gradient variation. Expected cell tip flattening would then drive two important consequences: tangential advection along interface would be weaker in the vicinity of cell tip; cell tip would move towards colder location in thermal field.

The first effect – reduction of tangential advection – implies both that disturbances generated at the tip have longer times to grow and that groove disturbances might more easily react back on cell tip to sustain feed-back oscillations [12]. In the first case, sidebranching should be *enhanced* according to noise amplification theory; in the latter case, it should be *enhanced* too according to oscillation theory.

The second effect, which results from solute conservation in steady growth state, refers to cell tip temperature. More precisely, flattening of cell tip is expected to drive cell tip position closer to planar front location, *i.e.* towards colder regions. Following this, cell tip undercooling should grow with thermal gradient, so that instability at cell tip, and, therefore, sidebranching, should be *enhanced*.

Finally, increasing thermal gradient is known to reduce the growth rate of the primary instability of planar fronts. Local stability of interface with respect to disturbance should thus be enhanced by raise of thermal gradient. This should tend to *inhibit* sidebranching.

Regarding sidebranching, increasing thermal gradient thus triggers both a stabilizing effect (through primary instability) and destabilizing effects (through cell tip flattening). The present experiment shows that the balance between these opposite tendencies goes towards destabilization, in agreement with the conclusion deduced from the evolution of sidebranching onset with control parameters (Fig. 1, [12]). However, further clarification of this issue and of the dominant mechanism responsible for sidebranching requires to reach, beyond the qualitative level, a quantitative comparison between theory and experiment. This would turn out implementing predictions of theories as to the evolution of sidebranching onset and comparing with the experimental determination of this critical surface [12]. This can hardly be done for oscillation theories owing to a lack of definite theoretical framework [3]. Regarding noise amplification theory, comparison can be done but only for linear amplification of cell tip disturbances and within a WKB approximation [6]. This will be presented elsewhere.

## 5 Conclusion

We have studied experimentally the effect of change of thermal gradient on sidebranch emission by growth cells in directional solidification of impure succinonitrile. *Enhancement* of sidebranching by *raise* of thermal gradient has been *directly* evidenced on cells. This corroborates an essential feature of sidebranching, *indirectly* deduced from its critical surface [12]. As the destabilizing effect of thermal gradient with respect to sidebranching is opposite to its stabilizing nature for planar fronts, our experimental observation implies that other factors than the primary instability of growth front play an essential role in the mechanism of sidebranch emission. Two candidates are cell shape and cell tip undercooling. Whether they could explain, not only qualitatively but also *quantitatively*, the dependence of the critical surface of sidebranching on thermal gradient, stands as a coupled experimental and theoretical challenge, capable of improving our understanding of this phenomenon.

## References

1. M.A. Eshelman, V. Seetharaman, R. Trivedi, *Acta Metall.* **36**, 1165 (1988); K. Somboonsuk, J.T. Mason, R. Trivedi, *Metall. Trans. A* **15**, 967 (1984).
2. E.A. Brener, M.B. Geilikman, D.E. Temkin, *Zh. Eksp. Teor. Fiz.* **94**, 241 (1988) [*Sov. Phys. JETP* **67**, 1002 (1988)].
3. J.S. Langer, H. Muller-Krumbhaar, *Phys. Rev. A* **27**, 499 (1983); O. Martin, N. Goldenfeld, *Phys. Rev. A* **35**, 1382 (1987).
4. P. Pelcé, A. Pumir, *J. Cryst. Growth* **73**, 337 (1985).
5. J.D. Weeks, W. van Saarloos, *Phys. Rev. A* **42**, 5056 (1990).
6. P. Pelcé, P. Clavin, *Europhys. Lett.* **3**, 907 (1987); J.S. Langer, *Phys. Rev. A* **36**, 3350 (1987); S.K. Sarkar, *Phys. Lett. A* **117**, 137 (1986).
7. C. Huang, M.E. Glicksman, *Acta Metall.* **29**, 701 (1981); A. Dougherty, P.D. Kaplan, J.P. Gollub, *Phys. Rev. A* **58**, 1652 (1987); Ph. Bouissou, A. Chiffaudel, B. Perrin, P. Tabeling, *Europhys. Lett* **13**, 89 (1990).
8. U. Bisang, J.H. Bilgram, *Phys. Rev. E* **54**, 5309 (1996).
9. M. Ben Amar, E. Brener, *Phys. Rev. Lett.* **71**, 589 (1993); E. Brener, *Phys. Rev. Lett.* **71**, 3653 (1993).
10. E. Brener, D. Temkin, *Phys. Rev. E* **51**, 351 (1995).
11. P. Mohlo, A.J. Simon, A. Libchaber, *Phys. Rev. A* **42**, 904 (1990); P. Kurowski, C. Guthmann, S. de Cheveigné, *Phys. Rev. A* **42**, 7368 (1990); X.W. Quian, H.Z. Cummins, *Phys. Rev. Lett.* **64**, 3638 (1990); L.M. Williams, M. Muschol, X. Quian, W. Losert, H.Z. Cummins, *Phys. Rev. E* **48**, 489 (1993).
12. M. Georgelin, A. Pocheau, *Phys. Rev. E* **57**, 3189-3204 (1998).
13. B. Billia, R. Trivedi, *Handbook of Crystal Growth*, Vol. 1, Chap. 14 (Elsevier Science Publishers, 1993).
14. J.D. Hunt, K.A. Jackson, H. Brown, *Rev. Sci. Instrum.* **37**, 805 (1966).
15. S. Akamatsu, G. Faivre, T. Ihle, *Phys. Rev. E* **51**, 4751 (1995).